Acta Crystallographica Section F
Structural Biology and Crystallization Communications
ISSN 1744-3091

Tyrosyl-tRNA synthetase: the first crystallization of a human mitochondrial aminoacyl-tRNA synthetase

Luc Bonnefond, Magali Frugier, Elodie Touzé, Bernard Lorber, Catherine Florentz, Richard Giegé,* Joëlle Rudinger-Thirion and Claude Sauter

Département 'Machineries Traductionnelles', Architecture et Réactivité de l'ARN, Université Louis Pasteur de Strasbourg, CNRS, IBMC, 15 Rue René Descartes, 67084 Strasbourg, France

Correspondence e-mail: r.giege@ibmc.u-strasbg.fr

Received 31 January 2007
Accepted 16 March 2007

Human mitochondrial tyrosyl-tRNA synthetase and a truncated version with its C-terminal S4-like domain deleted were purified and crystallized. Only the truncated version, which is active in tyrosine activation and *Escherichia coli* $tRNA^{Tyr}$ charging, yielded crystals suitable for structure determination. These tetragonal crystals, belonging to space group $P4_32_12$, were obtained in the presence of PEG 4000 as a crystallizing agent and diffracted X-rays to 2.7 Å resolution. Complete data sets could be collected and led to structure solution by molecular replacement.

1. Introduction

Aminoacyl-tRNA synthetases (aaRSs) are ancient enzymes that ensure the correct attachment of amino acids on tRNA 3′ ends. Each amino acid has its specific synthetase; there are therefore 20 aaRSs in nature, divided into two classes of ten based on structural and functional features of their catalytic domain (Cusack *et al.*, 1990; Eriani *et al.*, 1990). Tyrosyl-tRNA synthetases (TyrRSs) are modular proteins that belong to the first class of synthetases, but have dimeric organization and a class II mode of tRNA recognition (Yaremchuk *et al.*, 2002). TyrRS from *Bacillus stearothermophilus* was the first synthetase to have its structure solved (Bhat *et al.*, 1982) and at present TyrRSs, with structures of representatives of the three kingdoms of life (Bedouelle, 2005) and even from the mimivirus infecting the protist *Acanthamoeba polyphaga* (Abergel *et al.*, 2005), are among the best-known aaRSs (Fig. 1). However, many features related to the function, phylogeny and structure of this family of enzymes remain to be deciphered. As far as function is concerned, TyrRSs are peculiar in the way they specify cognate tRNA recognition. While major identity elements in tRNA for recognition by

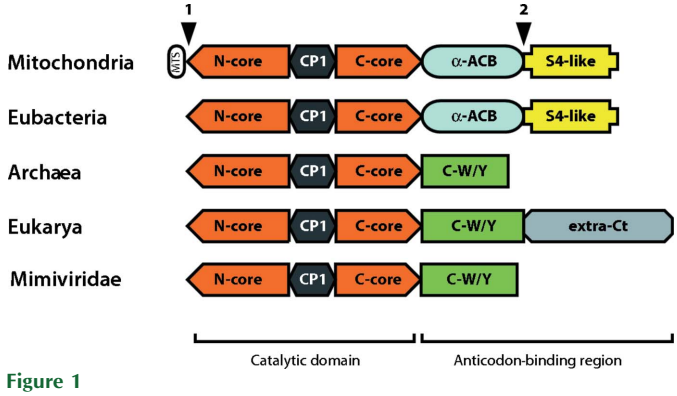

Figure 1
Structural organization of mitochondrial TyrRSs compared with their homologues in the three domains of life and in mimivirus. Each structural domain is displayed in a different colour. Abbreviations are MTS, mitochondrial target sequence; N-core and C-core, N and C parts of the catalytic domain, respectively; CP1, connective peptide; α-ACB, α-helical anticodon-binding domain; C-W/Y, C-terminal domain homologue to TrpRS; S4-like, ribosomal protein S4-like domain; extra-Ct, additional C-terminal domain. The full-length version of human mt-TyrRS (458 residues) was overexpressed without the MTS extension (arrow 1) and the truncated enzyme (356 residues) was overexpressed after further removal of the C-terminal S4-like domain (arrow 2). Notice that only one mimivirus is known; it codes for a TyrRS that resembles archaeal TyrRSs (Abergel *et al.*, 2005).

aaRSs have mostly been conserved in evolution (Giegé *et al.*, 1998), this is not the case in the tyrosine system. The major determinant, namely base pair N1–N72 at the top of the $tRNA^{Tyr}$-accepting branch, is G–C in bacteria/mitochondria but C–G in archaea/eukarya. Moreover, for reasons that are still unclear, base pair G1–C72 has lost its functional role in human mitochondria and most likely also in other vertebrate mitochondria (Bonnefond, Frugier *et al.*, 2005). To date, structural knowledge of mitochondrial aaRSs is limited to only two enzymes, namely TyrRS from *Neurospora crassa* (Paukstelis *et al.*, 2005) and bovine SerRS (Chimnaronk *et al.*, 2004). Our interest in mitochondrial aaRSs (Bonnefond, Fender *et al.*, 2005) also stems from the structural and functional peculiarities of mitochondrial tRNA aminoacylation systems compared with their cytoplasmic homologues (Sissler *et al.*, 2005) and, in the particular case of human mitochondria, from the correlations between pathologies and defects in the translational machinery (Florentz *et al.*, 2003; Jacobs & Turnbull, 2005). For all these reasons, we focused our attention on TyrRS from *Homo sapiens* mitochondria, a protein that shows 37% sequence identity with the most closely related TyrRS of known structure, namely that from *B. stearothermophilus*. Here, we report the crystallization and X-ray crystallographic studies of this human TyrRS in its full-length (human mt-TyrRS) and C-terminally truncated (human mt-TyrRS-ΔS4) versions.

2. Material and methods

2.1. Cloning, overproduction and protein characterization

Two forms of human mt-TyrRS were produced: the full-length protein and a truncated form lacking the S4-like domain (Fig. 1). Full-length TyrRS was cloned as described in Bonnefond, Fender *et al.* (2005). The truncated version was cloned following the same procedure using the pQE70-mt-TyrRS plasmid as PCR template (primers were 5′-ATG CGA **GGA TCC** CAC TCG GGC GCT CAG GGG-3′ and 5′-GGT GGT **AGA TCT** GTG ATA AAG GGC TTG TGT ACA CC-3′, with *Bam*HI and *Bgl*II restriction sites in bold). The cloning vector introduced a tetrapeptide (MRGS) and a His-tagged octapeptide (RSH_6) at the N- and C-terminal extremities of the cloned TyrRSs, respectively. The overproduction and purification procedures were similar for both proteins and were adapted with minor modifications from Bonnefond, Fender *et al.* (2005). In brief, top10 *Escherichia coli* strains containing either pQE70-mt-TyrRS or pQE70-mt-TyrRS-ΔS4 were grown in LB medium at 310 K until an OD_{600} of 0.7 was reached. Protein expressions were induced overnight at 298 K with 500 µ*M* IPTG. After centrifugation, cell pellets were suspended in 25 ml buffer *A* [50 m*M* NaH_2PO_4 pH 8.0, 300 m*M* NaCl, 5 m*M* dithioerythritol (DTE)] and sonicated six times for 45 s on ice. Lysed cells were centrifuged at 35 000*g* for 30 min at 277 K and the supernatants were loaded onto a 2 ml Ni–NTA column (Qiagen). Proteins were eluted with an imidazole gradient (20–500 m*M*). The pooled enzyme-containing fractions were dialyzed and concentrated for 3 h at 277 K against buffer *B* (50 m*M* HEPES–NaOH pH 6.7, 300 m*M* NaCl, 10 m*M* DTE) with 50% glycerol. Two further dialyses for 2 h against buffer *B* with 10% glycerol and then overnight against buffer *B* gently removed glycerol with minimal volume change. About 5 mg (at ∼2–3 mg ml^{-1}) full-length or 25 mg (at ∼6 mg ml^{-1}) truncated electrophoretically pure human mt-TyrRSs were recovered from 1 l LB medium.

The protein particle weight and polydispersity were determined on the basis of size-exclusion chromatography (SEC) and dynamic light-scattering (DLS) measurements. SEC analyses were performed at 277 K on an analytical 15 ml Bio-Prep SE-100/17 column (Bio-Rad) equilibrated in buffer *B*. The TyrRS elution volume was compared with those of proteins of known molecular weights and hydrodynamic radius. DLS analyses were performed at 293 K on 12 µl protein samples at appropriate concentration using a DynaPro DP801

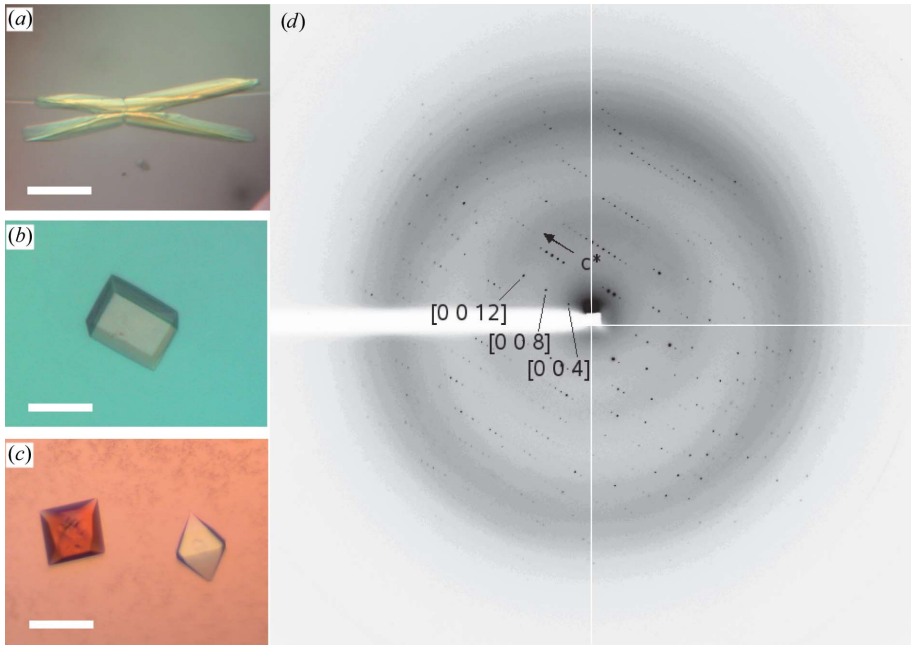

Figure 2
Crystals and diffraction properties of human mt-TyrRS. (*a*) Needles of full-length mt-TyrRS grown in 2 *M* ammonium sulfate pH 6.5, 10% glycerol, 0.1 *M* magnesium sulfate. (*b*) Prismatic crystals of truncated mt-TyrRS-ΔS4 in 18%(*w*/*v*) PEG 4000, 120 m*M* ammonium acetate, 0.1 *M* Tris–sodium citrate pH 5.6. (*c*) Bipyramidal crystals of mt-TyrRS-ΔS4 in 30%(*w*/*v*) PEG 4000, 0.2 *M* ammonium acetate, 0.1 *M* sodium acetate pH 4.6. The bars in (*a*), (*b*) and (*c*) correspond to 100 µm. (*d*) Diffraction pattern of a bipyramidal crystal. The image consists of a 0.5° oscillation. The resolution at the corner and the edge of the ADSC Quantum Q210 detector is 2.0 and 2.6 Å, respectively. Reflections of the [00*l*] row (see indices) indicate the presence of a helicoidal fourfold axis along the *c*/*c** direction.

instrument (Protein Solutions Inc.). Diffusion coefficients, particle radii and weights were corrected for buffer viscosity and refractive index. Other protein-characterization techniques (SDS–PAGE and N-terminal sequencing) were performed using standard methods. TyrRS activities were determined as described in Bonnefond, Fender *et al.* (2005).

2.2. Protein crystallization and crystal analysis

Crystallization trials were set up at 293 K in 96-well plates (Greiner) using a Mosquito robot (TTP LabTech Ltd). Sitting drops of 600 nl–2 µl (1:1 to 4:1 mixtures of 3–6 mg ml^{-1} protein in buffer *B* and reservoir solutions) were equilibrated by vapour diffusion against 80 µl reservoir solution. Prefilled screens (Qiagen) were employed with both full-length and truncated mt-TyrRS. Crystals of either enzyme form grew in about two weeks. They were mounted in cryoloops (Hampton Research), their mother liquor replaced with Paratone (Hampton Research) and flash-frozen in a nitrogen stream. Two data sets for truncated TyrRS were successfully collected to 3.2 and 2.7 Å resolution at 93 K on the ID14-EH4 or ID14-EH1 beamlines at ESRF, France equipped with an ADSC Quantum 315 or 210 CCD detectors, respectively. Data were processed with the *HKL* package (Otwinowski & Minor, 1997).

3. Results and discussion

3.1. Purification, stability and crystallization of full-length human mt-TyrRS

Purification of full-length human mt-TyrRS (103 kDa, 2 × 458 residues) resulted in pure and active protein (Bonnefond, Fender *et al.*, 2005). Migration of the pure protein on an SDS gel under reducing conditions with DTE in the loading buffer revealed a single band corresponding to the intact monomer, as confirmed by N-terminal sequencing. DLS measurements indicated the protein to be polydisperse and gave a mean hydrodynamic radius of 54 Å, in agreement with the expectation that the enzyme forms an elongated dimer. This enzyme has a tendency to aggregate and to lose its activity at concentrations above 2 mg ml^{-1}.

Extensive crystallization assays, conducted with fresh protein samples at 2 mg ml^{-1}, led to needle-like crystals (Fig. 2*a*) that diffracted X-rays poorly. Their quality could not be improved. Further assays with the enzyme complexed to *E. coli* tRNA^{Tyr} (as verified by DLS analysis) were also ineffective in producing crystals suitable for structure determination. Similar observations were reported for the mitochondrial TyrRS from *N. crassa* (Paukstelis *et al.*, 2005).

3.2. Towards high-quality crystals

As was performed with *E. coli* (Kobayashi *et al.*, 2005), *Staphylococcus aureus* (Qiu *et al.*, 2001) and mitochondrial *N. crassa* TyrRSs (Paukstelis *et al.*, 2005), the C-terminal domain of human mt-TyrRS, which is likely to be floppy, was removed. This domain, which is analogous to ribosomal protein S4, was delimited by multiple sequence alignment with bacterial TyrRSs and assigned as the 102 last residues (Fig. 1). The truncated version therefore encompasses the N-terminal catalytic domain and the anticodon-binding domain.

The purified truncated TyrRS migrates as a unique 40 kDa band on SDS gel, activates tyrosine and charges *E. coli* tRNA^{Tyr}. This protein (2 × 356 residues) is monodisperse in DLS, with a mean hydrodynamic radius of 38 Å, in agreement with a homodimeric structure. This conclusion was confirmed by SEC analyses. Importantly, deletion of the S4-like domain significantly increases the solubility of the synthetase, which can now be concentrated up to 20 mg ml^{-1}, thus opening new crystallization possibilities.

Table 1
X-ray analysis of a human mt-TyrRS-ΔS4 crystal.

Data were collected from a bipyramidal crystal (see Fig. 2*c*); values in parentheses are for the highest resolution shell.

Beamline	ID14-1, ESRF
Wavelength (Å)	0.934
Space group	$P4_32_12$
Unit-cell parameters (Å)	a = 78.8, c = 121.1
Crystal mosaicity (°)	0.7
Resolution range (Å)	2.7–30 (2.7–2.8)
No. of observations	534152
No. of unique reflections	11044
Completeness (%)	99.9 (100)
Multiplicity	13.1 (13.3)
R_{merge}† (%)	6.8 (37.2)
$\langle I/\sigma(I)\rangle$	27.8 (4.9)
Matthews coefficient (Å^3 Da^{-1})	2.4
Solvent content (%)	48
Asymmetric unit content	1 monomer

† $R_{merge} = \sum_{hkl}\sum_i |I_i(hkl) - \langle I(hkl)\rangle| / \sum_{hkl}\sum_i I_i(hkl)$.

More than 600 different crystallization conditions were assayed with human mt-TyrRS-ΔS4, of which 40 gave crystals. Most of them contained PEGs as the crystallizing agent. The largest crystals display prismatic and bipyramidal morphologies (Figs. 2*b* and 2*c*). The better diffracting bipyramidal crystals (Fig. 2*c*) grew reproducibly at pH 4.6 and in the presence of 30%(*w*/*v*) PEG 4000. By changing the protein:precipitant ratio to 2:1, their dimensions were enlarged and their diffraction limit extended from 3.2 to 2.7 Å.

3.3. Preliminary X-ray data

Crystals of truncated TyrRS were analyzed using synchrotron radiation. Statistics and other crystallographic data for the best crystal are given in Table 1. Based on systematically absent reflections, the space group is either $P4_32_12$ or $P4_12_12$ (Fig. 2*d*). Analysis of the solvent content performed with the *CCP*4 package (Collaborative Computational Project, Number 4, 1994) gave a unique solution consistent with one polypeptide chain (356 residues) per asymmetric unit. Molecular-replacement (MR) trials were performed with the *CaspR* MR webservice (Claude *et al.*, 2004) using the structure of *E. coli* TyrRS (PDB code 1wq3) and derived search models. In the resolution range 3–15 Å, space group $P4_32_12$ gave a better solution (correlation = 52%, *R* factor = 53%) than its enantiomorph $P4_12_12$ (correlation = 46%, *R* factor = 56%). Notice that the subunits of the biological dimer are related by the crystallographic twofold symmetry axis. After rigid-body refinement, the MR solution led to an interpretable electron-density map. Refinement of the model is in progress.

The authors acknowledge the teams at the ID14 beamlines at ESRF (Grenoble, France) for assistance during data collection as well as Guillaume Bec for help with the nanodrop crystallization robot and Marie Sissler for stimulating discussions. This work was supported by the Centre National de la Recherche Scientifique, Université Louis Pasteur (Strasbourg) and by grants from the French Ministry for Research (ACI-BCMS 042358). LB was supported by a grant from the French Ministry for Research and CS was the recipient of a Marie Curie European Reintegration Grant (MERG-CT-2004-004898).

References

Abergel, C., Chenivesse, S., Byrne, D., Suhre, K., Arondel, V. & Claverie, J.-M. (2005). *Acta Cryst.* F**61**, 212–215.

Bedouelle, H. (2005). *Aminoacyl-tRNA Synthetases*, edited by M. Ibba, C. Francklyn & S. Cusack, pp. 111–124. Georgetown, TX, USA: Landes Biosciences.

Bhat, T. N., Blow, D. M., Brick, P. & Nyborg, J. (1982). *J. Mol. Biol.* **158**, 699–709.

Bonnefond, L., Fender, A., Rudinger-Thirion, J., Giegé, R., Florentz, C. & Sissler, M. (2005). *Biochemistry*, **44**, 4805–4816.

Bonnefond, L., Frugier, M., Giegé, R. & Rudinger-Thirion, J. (2005). *RNA*, **11**, 558–562.

Chimnaronk, S., Jeppesen, M. G., Shimada, N., Suzuki, T., Nyborg, J. & Watanabe, K. (2004). *Acta Cryst.* D**60**, 1319–1322.

Claude, J.-B., Suhre, K., Notredame, C., Claverie, J.-M. & Abergel, C. (2004). *Nucleic Acids Res.* **32**, W606–W609.

Collaborative Computational Project, Number 4 (1994). *Acta Cryst.* D**50**, 760–763.

Cusack, S., Berthet-Colominas, C., Härtlein, M., Nassar, N. & Leberman, R. (1990). *Nature (London)*, **347**, 249–255.

Eriani, G., Delarue, M., Poch, O., Gangloff, J. & Moras, D. (1990). *Nature (London)*, **347**, 203–206.

Florentz, C., Sohm, B., Tryoen-Tóth, P., Pütz, L. & Sissler, M. (2003). *Cell. Mol. Life Sci.* **60**, 1356–1375.

Giegé, R., Sissler, M. & Florentz, C. (1998). *Nucleic Acids Res.* **26**, 5017–5035.

Jacobs, H. & Turnbull, D. (2005). *Trends Genet.* **21**, 312–314.

Kobayashi, T., Takimura, T., Sekine, R., Vincent, K., Kamata, K., Sakamoto, K., Nishimura, S. & Yokoyama, S. (2005). *J. Mol. Biol.* **346**, 105–117.

Otwinowski, Z. & Minor, W. (1997). *Methods Enzymol.* **276**, 307–326.

Paukstelis, P. J., Coon, R., Madabusi, L., Nowakowski, J., Monzingo, A., Robertus, J. & Lambowitz, A. M. (2005). *Mol. Cell*, **17**, 417–428.

Qiu, X., Janson, C. A., Smith, W. W., Green, S. M., McDevitt, P., Johanson, K., Carter, P., Hibbs, M., Lewis, C., Chalker, A., Fosberry, A., Lalonde, J., Berge, J., Brown, P., Houge-Frydrych, C. S. V. & Jarvest, R. L. (2001). *Protein Sci.* **10**, 2008–2016.

Sissler, M., Pütz, J., Fasiolo, F. & Florentz, C. (2005). *Aminoacyl-tRNA Synthetases*, edited by M. Ibba, C. Francklyn & S. Cusack, pp. 271–284. Georgetown, TX, USA: Landes Biosciences.

Yaremchuk, A., Kriklivyi, I., Tukalo, M. & Cusack, S. (2002). *EMBO J.* **21**, 3829–3840.